M.B. Yilmaz, A. Klein, and L. Xiang, ”Completion Time Minimization for UAV-aided Communications with Rotatable Dipole Array”, in *IEEE International Conference on Communications (ICC)*, Montreal, Canada, June 2025.

Completion Time Minimization for UAV-aided Communications with Rotatable Dipole Array

Mustafa Burak Yilmaz, Anja Klein, and Lin Xiang
Communications Engineering Lab, Technical University of Darmstadt, Darmstadt, Germany
Email: {b.yilmaz, a.klein, l.xiang}@nt.tu-darmstadt.de

***Abstract*—This paper investigates UAV-aided wireless communications with multiple users while utilizing a rotatable dipole array at the UAV. We jointly optimize user scheduling, array steering, and beamforming to minimize the UAV's mission completion time, i.e., the time required to deliver a specified data volume from the UAV to each user. To tackle the resulting nonconvex mixed-integer nonlinear program (MINLP) problem, we identify a hidden convexity in the optimization of continuous variables for given values of the discrete variables. Leveraging this result, we reformulate the original problem as a multi-stage dynamic programming (DP) problem and characterize its optimal solution via the Bellman optimality equation. We further propose a novel low-complexity one-step lookahead rollout (OSLR) algorithm based on approximate DP and semidefinite programming (SDP) jointly to optimize the discrete and continuous variables, respectively. Simulation results demonstrate that our proposed algorithm achieves significant reductions in the UAV's mission completion time compared to two baseline schemes, even when only a small number of dipoles are deployed at the UAV.**

I. Introduction

Multi-antenna unmanned aerial vehicles (UAVs) have emerged as a crucial technology to swiftly address both standard and emergency wireless communication demands by serving as aerial base stations (BSs), relays, or access points (APs) [1]. Through beamforming and precoding, the elevated antennas onboard UAVs enable spectral-efficient signal transmission and reception, while mitigating potential line-of-sight (LoS) interference. Furthermore, UAVs can proactively avoid blockages and reduce path losses via movements, to enhance wireless channel quality, even in complex urban environments.

However, unlike ground BSs and APs, UAVs often face size, weight, and power constraints, which severely limits the number of antennas they can carry, and consequently their communication performance. To overcome this limitation, extensive research has focused on joint beamforming and trajectory optimization for multi-antenna UAVs [2], with recent studies extending to cooperative beamforming and trajectory design for UAV swarms [3], [4]. Compact mmWave antenna arrays have also been explored in [5], to meet the deployment constraints. However, these studies often assume isotropic models for antenna elements, which overlook the three-dimensional (3D) radiation patterns of real-world antennas [6].

Recent work has addressed this gap by exploring practical (arrays of) directional antennas, such as half-wavelength dipoles and patch antennas [1]. In our prior research [7], [8], we extended this approach by employing UAV rotation or gimbals to steer the 3D orientation of antenna arrays. This approach, along with beamforming, enables highly directive beam shaping that focuses signals toward target areas while reducing interference. As a result, it achieves high spectral efficiency [7] and energy efficiency [8], even with a limited number of antennas. Additionally, this technique has been applied to integrated sensing and communication (ISAC) in [9], [10]. However, these studies assume simultaneous transmission to all users (and targets in ISAC), which may not be optimal when users spread across a wide spatial range. In such cases, the presence of users outside the main lobe of directional antennas can severely degrade the performance gains of rotatable antenna array. Moreover, previous studies assume *continuous* array steering, optimized using manifold optimization, whereas practical implementation often necessitates discrete array steering. Simple quantization of continuous optimization results, however, is known to be suboptimal.

To generalize our previous work [7]–[10] to diverse user distributions, in this paper, we explore joint *user scheduling* with array steering and beamforming for UAV-aided communications using a rotatable dipole array, specifically a uniform linear array (ULA) of half-wavelength dipoles. Unlike [7]–[10], we adopt *discrete* array steering and schedule users into multiple steering angles. To evaluate the performance limits of our proposed scheme, we jointly optimize user scheduling, array steering and beamforming to minimize mission completion time, i.e., the time required for the UAV to deliver a given data volume to each user [11]. Note that prior work on completion time minimization has usually focused on single-antenna transmitters, whose approaches are not applicable for our problem. For tractability, we employ zero-forcing (ZF) beamforming, which leads to a mixed-integer nonlinear programming (MINLP) problem. By reformulating the problem as a dynamic programming (DP) problem, we characterize its optimal solution via the Bellman optimality equation [12] and further propose a low-complexity approximate DP algorithm to derive an efficient suboptimal solution [13]. Our contributions are

- We present the first framework to jointly optimize user scheduling, discrete array steering, and ZF beamforming for completion time minimization in UAV-aided communication using a rotatable dipole array.
- We reveal a hidden convexity in the continuous optimization subproblem underlying the resulting MINLP, for fixed discrete variables. Leveraging this result, we reformulate the problem as a DP and characterize its optimal solution via the Bellman optimality equation.

This work has been funded by the LOEWE initiative (Hesse, Germany) within the emergenCITY center under grant LOEWE/1/12/519/03/05.001(0016)/72 and has been supported by the BMBF project Open6GHub under grant 16KISKO14 and by DAAD with funds from the German Federal Ministry of Education and Research (BMBF).

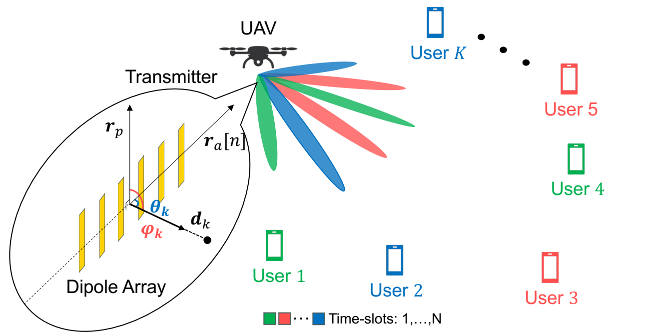

Fig. 1. Illustration of UAV-enabled communication using a rotatable dipole array and user scheduling.

We further propose a low-complexity approximate DP algorithm based on one-step lookahead rollout (OSLR) to achieve a high-quality solution.

- Simulation results demonstrate that the proposed OSLR algorithm achieves a significant reduction in completion time for UAV-aided communication compared to several baseline schemes, thanks to joint optimization of user scheduling, array steering, and ZF beamforming.

In this paper, matrices are denoted by boldface uppercase letters, and vectors by boldface lowercase letters. The symbols $\mathbf{A}^{\mathsf{T}}$, $\mathbf{A}^{\mathsf{H}}$, $\text{Rank}(\mathbf{A})$, and $\text{Tr}(\mathbf{A})$ denote the transpose, Hermitian, rank, and trace of the matrix $\mathbf{A}$, respectively. Additionally, $|\cdot|$ represents the absolute value of a complex scalar, and $\|\cdot\|$ represents the Euclidean norm of a vector.

II. System Model

This section presents the system model, including channel and signal models, and achievable data rate for UAV-aided communication using a rotatable dipole array.

A. UAV-aided Communication using Rotatable Dipole Array

As illustrated in Fig. 1, we consider a downlink communication system enabled by a rotary-wing UAV. The UAV is equipped with a uniform linear array (ULA) composed of S half-wavelength dipole antennas and serves as an aerial BS for sending messages to K downlink users scattered in a target area. User k is located at $\mathbf{u}_k \in \mathbb{R}^{3\times 1}$, $k \in \{1, \ldots, K\}$, and the users' locations are known to the UAV a priori. Each user is equipped with a single isotropic receive antenna, and we assume $S \geq K$. Moreover, the UAV hovers at a fixed location $\mathbf{u}_0 \in \mathbb{R}^{3\times 1}$ while serving the users.

The system operates in N time slots, indexed by $n = 1, \cdots, N$, where time slot n has a duration of $\tau[n] \geq 0$. The dipole ULA can be rotated in each time slot n to an angle selected from a discrete set $\mathcal{V}$ of orientations. For fast completion of the mission, we incorporate intelligent user scheduling in each time slot. As such, the hovering UAV can flexibly adjust the orientation and, jointly with beamforming and user scheduling, the shape of generated beams according to the communication needs of all users in the area of interest. Let $\alpha_k[n] \in \{0, 1\}$ be the user scheduling variable, where $\alpha_k[n] = 1$ if user k is scheduled for communication in time slot n and $\alpha_k[n] = 0$ otherwise. The direction of the dipole ULA in time slot n is denoted by a unit vector $\mathbf{r}_a[n] \in \mathbb{R}^{3\times 1}$, which is perpendicular to the dipoles of the ULA. The UAV's rotation axis is denoted by a unit vector $\mathbf{r}_p \in \mathbb{R}^{3\times 1}$ and aligned with the z-axis. This axis is orthogonal to $\mathbf{r}_a[n]$, where $\mathbf{r}_a[n] \cdot \mathbf{r}_p = 0$, as shown in Fig. 1.

B. Channel and Signal Models for Beamforming Transmission

The elevated UAV is assumed to be able to establish LoS links to the users. Consequently, we model the channel vector $\mathbf{h}_k[n]$ in time slot n from the UAV to user k as

$$\mathbf{h}_k[n] = \frac{\sqrt{\beta}}{\|\mathbf{u}_k - \mathbf{u}_0\|} \cdot \mathbf{a}_k[n], \tag{1}$$

where β represents the channel power gain at a unit distance and $\mathbf{a}_k[n] \in \mathbb{C}^{S\times 1}$ is the array steering vector in time slot n toward user k.

To define the steering vector $\mathbf{a}_k[n]$ for the considered rotatable dipole ULA, let us introduce a unit direction vector $\mathbf{d}_k \triangleq \frac{\mathbf{u}_k - \mathbf{u}_0}{\|\mathbf{u}_k - \mathbf{u}_0\|}$, which captures the direction from the UAV to user k. Additionally, we define the azimuth angle $\theta_k[n]$ as the angle formed by $\mathbf{r}_a[n]$ and $\mathbf{d}_k$, and the elevation angle φ_k as the angle formed between $\mathbf{r}_p$ and $\mathbf{d}_k$, respectively. Then, it follows from trigonometry that

$$\theta_k[n] = \arccos(\mathbf{d}_k^{\mathsf{T}} \mathbf{r}_a[n]), \tag{2}$$

$$\varphi_k = \arccos(\mathbf{d}_k^{\mathsf{T}} \mathbf{r}_p). \tag{3}$$

Using these notations, the steering vector $\mathbf{a}_k[n]$ is given as

$$\mathbf{a}_k[n] = \text{EF}(\varphi_k) \cdot [1, e^{\frac{j2\pi d}{\lambda}\cos(\theta_k[n])}, \ldots, e^{\frac{j2\pi(S-1)d}{\lambda}\cos(\theta_k[n])}]^{\mathsf{T}}, \tag{4}$$

where $\text{EF}(\varphi_k)$ characterizes the directional dependence of the radiated electric field of each dipole in a closed-form expression given by,

$$\text{EF}(\varphi_k) = \psi \cdot \frac{\cos(\frac{\pi}{2}\cos(\varphi_k))}{\sin(\varphi_k)}, \tag{5}$$

and ψ is a normalization factor to limit the total radiated power, such that $\int_0^{2\pi}\int_0^{\pi} EF^2(\varphi_k) \mathrm{d}\varphi_k \mathrm{d}\theta_k = 1$.

Let $c_k \in \mathbb{C}$ be the information bearing symbol intended for user k. We assume that c_k is a zero-mean complex Gaussian random variable with unit variance. Moreover, let $\mathbf{w}_k \in \mathbb{C}^{S\times 1}$ be the UAV's beamforming vector used for sending c_k. The resulting transmit signal of the UAV in time slot n is given as $\mathbf{x}[n] = \sum_{k=1}^{K} \mathbf{w}_k[n]\, c_k[n]$. The received signal at user k in time slot n is given as

$$y_k[n] = \sum_{i=1}^{K} (\mathbf{h}_k[n])^{\mathsf{H}} \mathbf{w}_i[n] c_i[n] + z_k[n], \tag{6}$$

where $z_k[n]$ is the noise generated at user k and is modeled as a zero-mean Gaussian random variable with variance σ_k^2. Based on (6), the achievable data rate $R_k[n]$ of user k in time slot n is given as

$$R_k[n] = B \log_2(1 + \gamma_k[n]), \tag{7}$$

$$\gamma_k[n] = \frac{|(\mathbf{h}_k[n])^{\mathsf{H}} \mathbf{w}_k[n]|^2}{\sum_{i=1, i\neq k}^{K} |(\mathbf{h}_k[n])^{\mathsf{H}} \mathbf{w}_i[n]|^2 + \sigma_k^2}, \tag{8}$$

where B is the system bandwidth and $\gamma_k[n]$ is the received signal-to-interference-plus-noise ratio (SINR) of user k.

III. Completion Time Minimization Problem

In this section, we employ the UAV with rotatable dipole array to deliver D_k bits to each user k. To efficiently utilize the rotatable dipole array and available radio resources for UAV-aided communication, we jointly optimize the UAV's transmit beamforming vectors $\{\mathbf{w}_k[n]\}$, the orientation of the dipole ULA $\{\mathbf{r}_a[n]\}$, user scheduling $\{\alpha_k[n]\}$, and time slot durations $\{\tau[n]\}$ to minimize the mission completion time, i.e., the time required to complete the data delivery, while ensuring QoS requirements for all users. For problem tractability, in this paper, we focus on zero-forcing (ZF) beamforming, which minimizes multiuser interference in (8). Note that ZF beamforming is widely recognized for its near-optimal performance in the high signal-to-noise regime, commonly encountered in UAV-aided communications. The resulting optimization problem is formulated as

$$\begin{aligned}
\text{P1}: & \min_{\mathbf{r}_a[n],\mathbf{w}_k[n],\alpha_k[n],\tau[n]} \sum_{n=1}^{N} \tau[n] \qquad (9)\\
\text{s.t. C1: } & \gamma_k[n] \geq \alpha_k[n]\gamma_{\min}, \ \ \forall k, \forall n\\
\text{C2: } & \sum_{n=1}^{N} R_k[n] \ \tau[n] \geq D_k, \ \forall k\\
\text{C3: } & \sum_{k=1}^{K} \mathrm{Tr}(\mathbf{w}_k[n]\mathbf{w}_k^{\mathsf{H}}[n]) \leq P_{\max}, \forall n\\
\text{C4: } & \mathrm{Tr}(\mathbf{w}_k[n]\mathbf{w}_k^{\mathsf{H}}[n]) \leq \alpha_k[n] \, P_{\max}, \forall k, \forall n\\
\text{C5: } & \sum_{i=1, i\neq k}^{K} \alpha_k[n] |\mathbf{h}_k^{\mathsf{H}}[n]\mathbf{w}_i[n]|^2 = 0, \forall n\\
\text{C6: } & \alpha_k[n] \in \{0,1\}, \ \ \forall k, \forall n\\
\text{C7: } & \tau[n] \geq 0, \ \ \forall n\\
\text{C8: } & \mathbf{r}_a[n] \in \mathcal{V}, \ \ \forall n.
\end{aligned}$$

In problem P1, C1 guarantees a minimum received SINR $\gamma_{\min}$ for scheduled communication users, i.e., for users satisfying $\alpha_k[n]=1$. For unscheduled users, C1 reduces to $\gamma_k[n] \geq 0$, which can be neglected without altering the feasible set of P1. C2 guarantees that each user k receives at least D_k bits in the considered N time slots. C3 limits the maximum transmit power of the dipole ULA to $P_{\max}$. C4 ensures that no transmit power is allocated to unscheduled users with $\alpha_k[n]=0$, as $\mathbf{w}_k[n] = \mathbf{0}$. C5 mitigates interferences to scheduled users, under the ZF beamforming. Similar to C1, for unscheduled users with $\alpha_k[n]=0$, C5 can be safely neglected. C6 is the binary constraint on user scheduling, where multiple users can be simultaneously scheduled in one time slot. Finally, C7 requires a nonnegative duration of each time slot and C8 limits the UAV's orientations to the discrete set $\mathcal{V}$.

Note that P1 is a nonconvex MINLP problem due to the discrete variables $\mathbf{r}_a[n]$ and $\alpha_k[n]$ in constraints C6 and C8, and the nonconvex constraints C1, C2, and C5. Moreover, there exist tight couplings between the direction $\mathbf{r}_a[n]$ of the dipole ULA and the transmit beamforming vector $\mathbf{w}_k[n]$, cf. (4) and (8), as well as between duration $\tau[n]$ and beamforming vector $\mathbf{w}_k[n]$, cf. C2. These obstacles render problem P1 generally intractable. In Sec. IV we overcome these challenges by reformulating P1 as a multi-stage DP, whose optimal solution is given by the Bellman optimality equation [12]. However, exactly solving this equation using standard DP algorithms has a prohibitive computational complexity. Inspired by the success of approximate DP and reinforcement learning, we propose a low-complexity, high-quality suboptimal algorithm based on the rollout method [13] to obtain an approximate solution to the Bellman equation.

IV. Proposed Solution

To facilitate the solution to problem P1, we divide its optimization variables into continuous and discrete groups, given by $\{\mathbf{w}_k, \tau[n]\}$ and $\{\mathbf{r}_a[n], \alpha_k[n]\}$, respectively. For given $\{\mathbf{r}_a[n], \alpha_k[n]\}$ in P1, we show in Sec. IV-A that the remaining continuous optimization problem has a hidden convexity and can therefore be efficiently solved. Building on this, we reformulate P1 as a multi-stage DP for optimal and efficient suboptimal solutions in Secs. IV-B and IV-C, respectively.

Note that the SINR expression in (8) and consequently, problem P1 would become invalid if some users are active only in a fraction of a time slot rather than the whole time slot. However, we can safely rule out this possibility in the following lemma.

Lemma 1: Let $\tau^*[n]>0$ be an optimal solution of problem P1. If N is sufficiently large, e.g. when $N \geq K$, the UAV should transmit to all scheduled users in time slot n for the whole duration of $\tau^*[n]$.

Proof: A detailed proof is omitted due to limited page space. Suppose the UAV transmits to some scheduled user k only for duration $\tau'[n] < \tau^*[n]$. If only user k is scheduled in time slot n, $\tau^*[n]$ is not the optimal time duration. Otherwise, one can reduce the transmit power for user k and allocate it to other scheduled users. This will strictly lower the completion time, contradicting again the optimality of $\tau^*[n]$. ∎

A. Optimization of Beamforming and Time Slot Duration

Given the ULA's orientation $\mathbf{r}_a[n]$ and user schedule $\alpha_k[n]$, the optimization of continuous-valued beamforming vectors $\mathbf{w}_k$ and time slot durations $\tau[n]$ is given as

$$\text{P2}: \min_{\mathbf{w}_k[n],\tau[n]} \sum_{n=1}^{N} \tau[n] \qquad (10)$$
$$\text{s.t. C1, C2, C3, C4, C5, C7.}$$

Problem P2 is still nonconvex due to constraints C1, C2, and C5. However, by employing suitable transformations, we reveal below an underlying convexity in P2, allowing its globally optimal solution to be computed in polynomial time.

1) Problem Transformation: We define a new variable $\mathbf{W}_k[n] \triangleq \tau[n]\mathbf{w}_k[n]\mathbf{w}_k^{\mathsf{H}}[n]$, where $\mathbf{W}_k[n] \succeq 0$ and $\mathrm{Rank}(\mathbf{W}_k[n]) \leq 1$. With $\mathbf{W}_k[n]$, C1 can be reformulated as:

$$\begin{aligned}
&\text{C1: } |(\mathbf{h}_k[n])^{\mathsf{H}}\mathbf{w}_k[n]|^2/\sigma_k^2 \geq \gamma_{\min} \quad \Longleftrightarrow\\
&\overline{\text{C1}}\text{: } \mathrm{Tr}(\mathbf{W}_k[n]\mathbf{H}_k[n]) \geq \alpha_k[n]\tau[n]\gamma_{\min}\sigma_k^2, \qquad (11)
\end{aligned}$$

where $\mathbf{H}_k[n] \triangleq \mathbf{h}_k[n](\mathbf{h}_k[n])^{\mathsf{H}}$. Note that interference terms vanish in (11) due to the ZF constraint in C5. Similarly, C2 is rewritten as

$$\overline{\text{C2}}\text{: } \sum_{n=1}^{N} B\tau[n]\log_2\left(1+\frac{\mathrm{Tr}(\mathbf{W}_k[n]\mathbf{H}_k[n])}{\tau[n]\,\sigma_k^2}\right) \geq D_k. \quad (12)$$

Thus, with fixed ULA direction $\mathbf{r}_a[n]$ and user schedule $\alpha_k[n]$, problem P2 can be equivalently reformulated as

$$\text{P3}: \min_{\mathbf{W}_k[n],\tau[n]} \sum\nolimits_{n=1}^{N} \tau[n] \quad (13)$$

$$\text{s.t. } \overline{\text{C1}}, \overline{\text{C2}}, \text{C7}, \overline{\text{C3}}\text{: } \sum\nolimits_{k=1}^{K} \text{Tr}(\mathbf{W}_k[n]) \le P_{\max}\tau[n], \forall n$$

$$\overline{\text{C4}}\text{: } \text{Tr}(\mathbf{W}_k[n]) \le \alpha_k[n]\tau[n]\, P_{\max}, \forall k, \forall n$$

$$\overline{\text{C5}}\text{: } \sum\nolimits_{i=1, i\neq k}^{K} \alpha_k[n]\text{Tr}(\mathbf{W}_k[n]\mathbf{H}_k[n]) = 0, \forall n$$

$$\text{C9: } \mathbf{W}_k[n] \succeq 0, \forall n, \forall k$$

$$\text{C10: } \text{Rank}(\mathbf{W}_k[n]) \le 1,\ \forall n, \forall k.$$

2) Hidden Convexity and Optimal Solution: Now, eliminating constraint C10 from P3 yields a relaxed yet convex semidefinite program (SDP) that can be solved using off-the-shelf solvers such as CVX [14]. While this relaxation typically provides a performance lower bound, we can show that the relaxed solution for $\mathbf{W}_k$ in P3 *always* has rank one, resulting in a relaxed objective value that matches the optimal value of P3. This result is verified offline by simulations.

Lemma 2: Suppose problem P3 is *strictly feasible*, meaning there exists a solution satisfying at least one of the constraints with strict inequality. Then, the optimal solution of $\mathbf{W}_k[n]$ obtained by SDP relaxation always has rank one. Moreover, the optimal beamforming solution for P3 is given by the principal eigenvector of $\mathbf{W}_k[n]/\tau[n]$ when $\tau[n]>0$.

Proof: We provide only a sketch of the proof. Assuming strict feasibility in P3, the convex SDP obtained by relaxing constraint C10 fulfills the Slater's condition and thus has strong duality. As a result, the Karush–Kuhn–Tucker (KKT) conditions are both sufficient and necessary for the optimal relaxed solutions. Following similar arguments as in [15, Theorem 2], we can show that the optimal solution of $\mathbf{W}_k[n]$ derived from the KKT conditions always has rank one. Thus, the optimal transmit covariance matrix of problem P3 is given by $\mathbf{W}_k[n]/\tau[n]$ given $\tau[n]>0$, which completes the proof. ■

B. DP based Optimal Solution of Problem P1

We now demonstrate that problem P1 can be reformulated as an equivalent N-stage DP problem with stages indexed by $n = 1, \dots, N$ and thereby optimally solved via DP algorithms.

1) DP Reformulation: Let $D_k[n]$ be the remaining data volume in bits to be transmitted to user k at the start of time slot n. The system state at stage n is defined by $\mathbf{o}_n \triangleq (D_1[n], \dots, D_K[n])^\mathsf{T}$, consisting of the remaining data volume in bits to be transmitted to all users at the start of time slot n. The initial state is given by $\mathbf{o}_1{=}(D_1, \dots, D_K)^\mathsf{T}$ and the terminal state, where required data volume is delivered to all users, is denoted as $\mathbf{o}_{N+1} = \mathbf{0}$. The action at stage n, represented by $\mathbf{z}_n = (\mathbf{r}_a[n], \boldsymbol{\alpha}[n], \boldsymbol{\Delta}[n])$, consists of the direction of the dipole ULA $\mathbf{r}_a[n]$, the communication schedule for all users $\boldsymbol{\alpha}[n] \triangleq [\alpha_1[n], \dots, \alpha_K[n]]$, and the data volume $\boldsymbol{\Delta}[n] \triangleq [\Delta_1[n], \dots, \Delta_K[n]]$ in bits to be transmitted to all users, where $\Delta_k[n]$ is the number of bits transmitted to user k in time slot n. Applying action $\mathbf{z}_n$ transitions the system state to $\mathbf{o}_{n+1}$ according to system equation $\mathbf{o}_{n+1} = f_n(\mathbf{o}_n, \mathbf{z}_n)$, specifically

$$\mathbf{o}_{n+1} = \min(\mathbf{o}_n - \boldsymbol{\Delta}[n], \mathbf{0}). \quad (14)$$

Meanwhile, a cost $g_n(\mathbf{z}_n) = \tau[n]$ is incurred for transition from $\mathbf{o}_n$ to $\mathbf{o}_{n+1}$ under action $\mathbf{z}_n$, accounting for the time duration of stage n. This cost can be optimized by solving the convex problem P3 with the discrete variables fixed according to $\mathbf{z}_n$, cf. Sec. IV-A.

The actions $\mathbf{z}_n$, $n{=}1, \dots, N$, over stages are determined by a policy $\pi{=}\{\mu_1, \dots, \mu_N\}$, where μ_n maps states $\mathbf{o}_n$ to actions $\mathbf{z}_n{=}\mu_n(\mathbf{o}_n)$. To reach terminal state $\mathbf{o}_{N+1}$ while starting from the initial state $\mathbf{o}_1$, the total cost of the UAV mission using policy π is given by $J_\pi(\mathbf{o}_1) = \sum_{n=1}^{N} g_n(\mathbf{z}_n)$, representing the completion time for UAV-aided communication. Thus, problem P1 is equivalent to finding the optimal policy π^* that minimizes $J_\pi(\mathbf{o}_1)$ [12].

2) Bellman Optimality Equation: Let $J^*_{n,\pi^*}(\mathbf{o}_n)$ be the optimal value function of state $\mathbf{o}_n$, evaluating the minimum cost to reach the terminal state $\mathbf{o}_{N+1}$ from $\mathbf{o}_n$. The optimal policy π^* is then determined by solving the Bellman optimality equation at each stage $n{=}1, \dots, N$ [12]:

$$J^*_{n,\pi^*}(\mathbf{o}_n) {=} \min_{\mathbf{z}_n \in \mathcal{Z}(\mathbf{o}_n)} [g_n(\mathbf{z}_n) {+} J^*_{n+1,\pi^*}(f(\mathbf{o}_n, \mathbf{z}_n))], \quad (15)$$

where $\mathcal{Z}(\mathbf{o}_n)$ is the feasible set of actions applicable at state $\mathbf{o}_n$. The exact solution to (15) can be obtained via the DP algorithm, which starts with solving problem $J^*_{N+1,\pi^*}(\mathbf{o}_{N+1})$ at the terminal state and then moves backwards to solve $J^*_{N,\pi^*}(\mathbf{o}_N), \dots, J^*_1(\mathbf{o}_1)$ stage-wise. The optimal policy is then reconstructed based on these optimal value functions.

However, the DP algorithm is prohibitively time-consuming as the size of the state space grows exponentially with the number N of stages [12]. This motivates the use of low-complexity approximation methods, such as the rollout algorithm [13], to approximately solve (15).

C. Proposed One-Step Lookahead Rollout (OSLR) Algorithm

The computation burden of the DP algorithm is dominated by calculating the optimal value function J^*_{n+1,π^*}. The proposed OSLR algorithm reduces this complexity by approximating J^*_{n+1,π^*} with the value function $\tilde{J}_{n+1,\tilde{\pi}}$ of a *base policy* $\tilde{\pi} = \{\tilde{\mu}_1, \dots, \tilde{\mu}_N\}$. This base policy $\tilde{\pi}$ can be a heuristic with an easy-to-compute cost function $\tilde{g}_n$, such that

$$\tilde{J}_{n+1,\tilde{\pi}}(\mathbf{o}_{n+1}) \triangleq \sum\nolimits_{i=n+1}^{N} \tilde{g}_i(\tilde{\mathbf{z}}_i) \quad (16)$$

for actions $\tilde{\mathbf{z}}_i{=}\tilde{\mu}_i(\mathbf{o}_i), i{=}n{+}1, \dots, N$. Replacing J^*_{n+1,π^*} in (15) with $\tilde{J}_{n+1,\tilde{\pi}}$, the OSLR algorithm selects action $\mathbf{z}_n^+$ as

$$\mathbf{z}_n^+ \in \underset{\mathbf{z}_n \in \mathcal{Z}(\mathbf{o}_n)}{\operatorname{argmin}} \left[g_n(\mathbf{z}_n) + \tilde{J}_{n+1,\tilde{\pi}}(f(\mathbf{o}_n, \mathbf{z}_n)) \right]. \quad (17)$$

Thus, rather than following base policy $\tilde{\pi}$ directly, the OSLR approach optimizes each action by balancing the immediate cost $g_n(\mathbf{z}_n)$ with the approximate long-term cost $\tilde{J}_{n+1}$. This guarantees performance improvement over the base policy while lowering computational demands [13].

TABLE I
SIMULATION PARAMETERS

Parameter	Notation/Value
User locations $\mathbf{u}_k = [x_k, y_k, z_k]$	$x_k, y_k \in [-800, 800]$m, $z_k = 0$m
User data volume requirements	$D_k \in [1.5, 6]$Mbits
Number of ULA elements	$S = 8$
Reference channel gain	$\beta = -30$ dB
Noise power	$\sigma_k^2 = -110$ dBm
Maximum transmit power	$P_{\max} = 30$ dBm
Bandwidth	$B = 1$MHz
Communication SINR	$\gamma_{\min,k} = 10$ dB

Algorithm 1 details the proposed OSLR algorithm. At each stage n, the action set $\mathcal{Z}(\mathbf{o}_n)$ is characterized based on the current state $\mathbf{o}_n$ and constraints in P1. Next, the approximate value function $\tilde{J}_{n+1,\tilde{\pi}}(\mathbf{o}_n, \mathbf{z}_n)$ is computed using the base policy $\tilde{\pi}$ for all actions $\mathbf{z}_n \in \mathcal{Z}(\mathbf{o}_n)$. The improved action $\mathbf{z}_n^+$ is selected solving of the convex problem P3. Finally, the state is updated with the action $\mathbf{z}_n^+$. This process iterates through N stages, providing a sequence of UAV orientations and user schedules that minimize the UAV's mission completion time.

Algorithm 1 Joint Beamforming, UAV Orientation and Scheduling Optimization with OSLR

1: **Input:** $N, \tilde{\pi}, \mathcal{V}, P_{\max}, \gamma_{\min}, \mathbf{u}_0, \{\mathbf{u}_k, D_k\}_{k=1}^K$
2: **for** $n = 1 : N$ **do** ▷ For each stage n
3: Initialize $\mathcal{Z}(\mathbf{o}_n)$ ▷ Constraints of P1
4: Calculate $\tilde{J}_{n+1,\tilde{\pi}}(f(\mathbf{o}_n, \mathbf{z}_n))$, $\forall \mathbf{z}_n \in \mathcal{Z}(\mathbf{o}_n)$
5: $\mathbf{z}_n^+ = \underset{\mathbf{z}_n \in \mathcal{Z}(\mathbf{o}_n)}{\operatorname{argmin}} \left[g_n(\mathbf{z}_n) + \tilde{J}_{n+1,\tilde{\pi}}(\mathbf{o}_n, \mathbf{z}_n) \right]$
6: Update system: $\mathbf{o}_{n+1} = f_n(\mathbf{o}_n, \mathbf{z}_n^+)$ ▷ Solve P3
7: **end for**
8: **Output:** $[\mathbf{z}_1^+, \ldots, \mathbf{z}_N^+]$, $J_1^+(\mathbf{o}_1)$.

V. SIMULATION RESULTS

The performance of the proposed algorithm is evaluated via simulations. The UAV hovers at $\mathbf{u}_0 = [0, 0, 100]$ and serves $K = 6$ users. The discrete set of orientations $\mathcal{V}$ consists of uniformly spaced values covering the entire range of 360° with an angular separation of 30°. We consider $N = 6$ time slots with variable durations. Unless otherwise stated, the simulation parameters are set as in Table I.

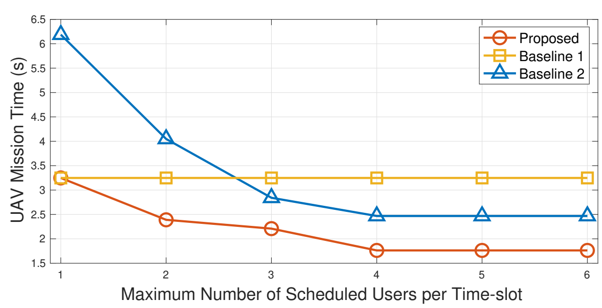

Fig. 2. UAV mission time versus maximum number of scheduled users per time slot.

To validate the effectiveness of Algorithm 1, we compare its performance against two baseline schemes.

- *Baseline Scheme 1:* This scheme estimates the UAV service time under the base policy alone, i.e., $\sum_{i=1}^{n} g_i(\tilde{\mathbf{z}}_i) + \tilde{J}_{n+1,\tilde{\pi}}(\mathbf{o}_n)$, where actions $\tilde{\mathbf{z}}_i$ are determined without OSLR improvement in (17).

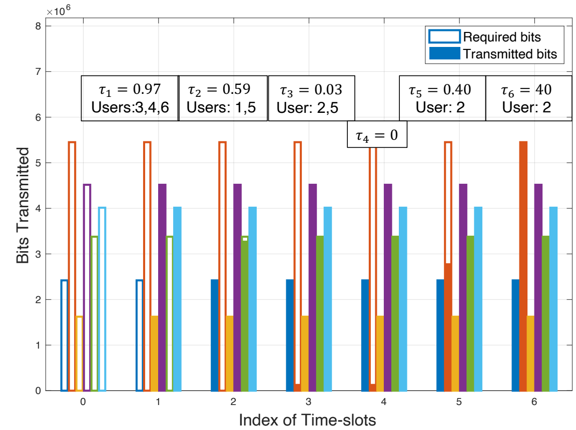

Fig. 3. Optimized time allocation and user scheduling of the proposed scheme, and the resulting progress of data delivery for each user over 6 time slots.

- *Baseline Scheme 2:* Unlike the proposed scheme, we optimize general linear beamforming by eliminating the ZF constraints C4 and C5 from P1. For tractability, C2 is modified into $\sum_{n=1}^{N} \alpha_k[n]\tau[n] \geq D_k / R_{\min}$, with $R_{\min} = B \log_2(1 + \gamma_{\min})$. This reformulation allows the resulting problem to be solvable with Algorithm 1, but optimizes user scheduling assuming $R_{\min}$ for each user.

Fig. 2 shows the UAV's mission completion time of the considered schemes when allowing only a maximum number of $K_s \leq K$ users to be simultaneously scheduled in each time slot. We observe that Baseline Scheme 1 is unaffected by K_s as it always serves only one user per time slot. For the proposed scheme and Baseline Scheme 2, the mission completion time first monotonically decreases with K_s, before saturating when $K_s \geq 4$. This is because as K_s increases but $K_s \leq 4$, more users can be simultaneously served within a time slot at high data rates. However, when $K_s > 4$, scheduling more than 4 users within a single time slot either becomes infeasible due to the minimum rate requirement for each scheduled user in constraint C1 of problem P1, or compromises the total throughput, given the wide spatial distribution of user locations and limited coverage range of the dipoles' main lobes.

For insights, Fig. 3 presents the optimized user scheduling and time durations of the proposed scheme, and the resulting progress of data delivery to each user, considering a ULA of S=6 antennas. We observe that all required data is successfully delivered in 5 out of 6 time slots, with the optimized durations for each time slot. The proposed scheme can exploit simultaneous communication with a small number users along the optimized ULA directions to accelerate the overall data delivery mission. Both Figs. 2 and 3 reveal that only a subset of the widely scattered users need to be scheduled per time slot for minimization of completion time. This can be exploited to reduce the search space for user scheduling and further lower the computational complexity of Algorithm 1, yet without degrading its performance.

Fig. 4 illustrates the UAV's mission time as a function of the communication SINR requirement per user, $\gamma_{\min}$, for the considered schemes. As expected, the mission time of Baseline Scheme 1 rarely changes for feasible SINR values,

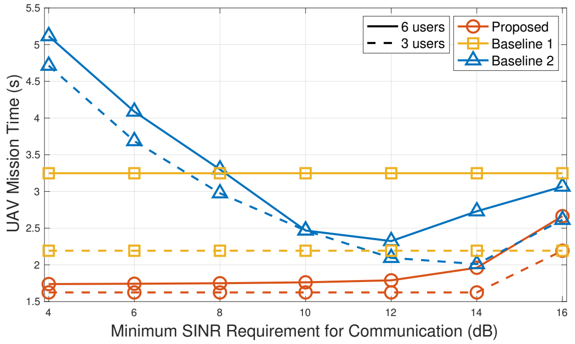

Fig. 4. UAV mission time versus the required communication SINR per user.

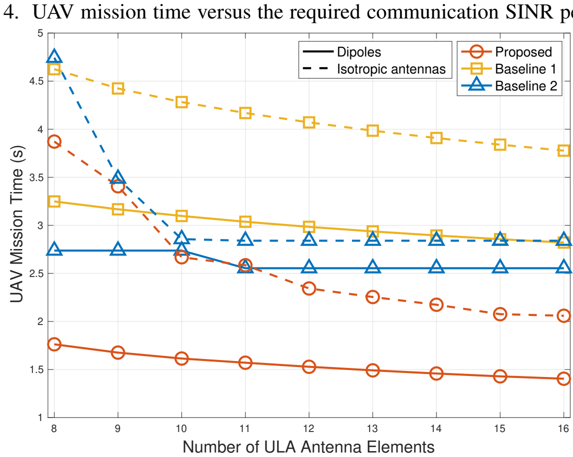

Fig. 5. UAV mission time versus the number of ULA antenna elements.

since it always serves a single user per time slot. With Baseline Scheme 2, the mission time initially decreases and then increases with $\gamma_{\min}$, where an optimal $\gamma_{\min}$ exists. This occurs because Baseline Scheme 2 schedules users based on their required minimum rate, $R_{\min}{=}B\log_2(1{+}\gamma_{\min})$, which is quite conservative for small values of $R_{\min}$. In such cases, the proposed scheme significantly outperform Baseline Scheme 2. In contrast, for large values of $R_{\min}$, both the proposed scheme and Baseline Scheme 2 can schedule only fewer users in the same time slot as $\gamma_{\min}$ increases, which unfavorably penalizes the mission time. Fig. 4 also reveals that, as the number of users increases from $K=3$ to $K=6$, the mission time of the proposed scheme only sees a modest increase for both $K=3$ and $K=6$ users (despite a larger data volume for 6 users).

Finally, Fig. 5 evaluates the UAV's mission time for different number of isotropic antennas and dipoles in the UAV's ULA. We observe that increasing the number S of antennas consistently improves the performance of all considered schemes, as it allows to focus the signal energy in narrower beams directed toward the users for achieving higher data rates. Baseline Scheme 2, however, achieves limited performance gains as S increases, since its $R_{\min}$-based scheduling policy becomes increasingly more conservative. In contrast, our proposed scheme achieves the best performance for both isotropic antennas and dipoles. This is because, through jointly optimizing user scheduling, ULA directions, time durations, and beamforming, the proposed scheme allows the UAV to better utilize the rotatable antenna array. Notably, when employing the rotatable dipole array, our proposed scheme significantly lowers the UAV's mission completion time even for $S=8$ antennas. This is because, even though both the dipole direction $\mathbf{r}_p$ and the elevation angle of each user φ_k remain unchanged, the proposed scheme can exploit the directional radiation pattern of dipole antennas, together with beamforming and horizontal array steering, to enhance the received signal of scheduled users while easily meeting the ZF beamforming constraint C5.

VI. Conclusions and Future Work

In this paper, we examined the joint optimization of transmit beamforming, user scheduling, and array orientation for UAV-aided wireless communications using a rotatable dipole ULA. We formulated a nonconvex MINLP problem for minimizing the UAV's mission time while satisfying the users' QoS requirements for communication. To tackle this problem, we reformulated it as a multi-stage DP problem and proposed a computationally efficient OSLR algorithm to obtain a high-quality suboptimal solution. Simulation results showed that the proposed scheme can effectively leverage the rotatable dipole ULA direction and user scheduling to significantly reduce the mission time required by the UAV for completing data delivery to the users. Given the promising performance and low complexity of the OSLR algorithm, future research will focus on extending it to support other base policies and multi-UAV systems, as well as for other UAV-enabled applications.

References

[1] W. Chen et al., "5G-advanced towards 6G: Past, present, and future", *IEEE J. Sel. Area Commun.*, vol. 41, no. 6, pp. 1592-1619, Jun. 2023.

[2] Q. Wu et al., "A comprehensive overview on 5G-and-beyond networks with UAVs: From communications to sensing and intelligence," *IEEE J. Sel. Areas Commun.*, vol. 39, no. 10, pp. 2912–2945, 2021.

[3] Q. Wu et al., "Joint Trajectory and Communication Design for Multi-UAV Enabled Wireless Networks," *IEEE Trans. Wireless Commun.*, vol. 17, no. 3, pp. 2109-2121, Mar. 2018.

[4] M. A. Khan, et al., "Swarm of UAVs for Network Management in 6G: A Technical Review," *IEEE Trans. Netw. Serv. Manag.*, vol. 20, no. 1, pp. 741-761, March 2023.

[5] Z. Xiao et al., "A survey on millimeter-wave beamforming enabled UAV communications and networking," *IEEE Commun. Surveys Tut.*, vol. 24, no. 1, pp. 557-610, 2021.

[6] C. A. Balanis, *Antenna Theory: Analysis and Design*. 4th ed, 2016.

[7] L. Xiang et al., "Joint Optimization of Beamforming and 3D Array Steering for Multi-antenna UAV Communications," in *Proc. IEEE WCNC*, Dubai, UAE, 2024.

[8] L. Xiang, et al., "Energy-Efficient Dynamic Array-Steering and Beamforming for UAV-Aided Communications," in *Proc. IEEE Globecom*, Cape Town, South Africa, Dec. 2024.

[9] F. Pei et al., "Joint Optimization of Beamforming and 3D Array-Steering for UAV-Aided ISAC," in *Proc. IEEE ICC*, Denver, Colorado, 2024.

[10] F. Pei et al., "Transmit Beamforming and Array Steering Optimization for UAV-Aided Bistatic ISAC", in *Proc. IEEE Globecom*, Cape Town, South Africa, Dec. 2024.

[11] T. Wang et al., "Safety Constrained Trajectory Optimization for Completion Time Minimization for UAV Communications," *IEEE Internet Things J.*, vol. 11, no. 21, pp. 34482-34491, Nov. 2024.

[12] D. P. Bertsekas, *Dynamic Programming and Optimal Control*, 4th ed. Athena Scientific, 2017, vol. 1 and 2.

[13] D. P. Bertsekas, *Lessons from AlphaZero for optimal, model predictive, and adaptive control*. Athena Scientific, 2022.

[14] M. Grant and S. Boyd, "CVX: Matlab software for disciplined convex programming, version 2.1," http://cvxr.com/cvx, Mar. 2014.

[15] J. Zhang et al., "Robust energy-efficient transmission for wireless-powered D2D communication networks," *IEEE Trans. Veh. Technol.*, vol. 70, no. 8, pp. 7951–7965, 2021.